https://doi.org/10.5194/egusphere-2026-4101
Preprint. Discussion started: 28 July 2026


# Limits on volcanic forcing of East Asian monsoon rainfall from the 247-year Seoul Chugugi precipitation record (1778–2024)

Seokhwan Hwang*, Heejun Park

*Korea Institute of Civil Engineering and Building Technology, Goyang 10223, Republic of Korea*

**Corresponding author. E-mail: sukany@kict.re.kr*

## Abstract

The 247-year Seoul precipitation record (1778–2024), comprising 130 years of daily Chugugi rain-gauge measurements (1778–1907; Lee et al., 2024) extended by modern instrumental observations (KMA station 108, 1908–2024), constitutes the longest pre-industrial daily rainfall record in the world. Here we exploit this archive to test whether the circumglobal-teleconnection (CGT) mechanism that has been proposed to connect tropical volcanic eruptions to East Asian monsoon drought (Nie et al., 2026) imprints detectably on Seoul summer (JJA) rainfall. We apply Superposed Epoch Analysis (SEA) over 9 major eruptions (1783 Laki through 2022 Hunga Tonga) with 5,000-sample Monte Carlo bootstrap significance, continuous Morlet wavelet spectral analysis with AR(1) red-noise testing, and extended wavelet coherence between annual global VEI ≥ 4 eruption counts and Seoul JJA rainfall over 1830–2024 (N = 195). Three findings emerge. (i) The composite SEA shows no statistically significant post-eruption rainfall response at any lag from 0 to +7 yr (composite tropical-only –65 mm to +76 mm across the window; $p > 0.45$ at every post-eruption lag). Individual eruptions divide roughly equally between wet and dry post-eruption responses: Tambora (+298 mm), Krakatau (+132 mm), Agung (+267 mm), and Katmai (+58 mm) show net-wet years +1 to +3, while Cosiguina (–245 mm), Santa Maria (–109 mm), El Chichón (–153 mm), Pinatubo (–184 mm), and Laki (–152 mm) show net-dry. (ii) Wavelet spectral analysis reveals two significant decadal-to-multidecadal modes above the AR(1) red-noise null: a quasi-40-yr Pacific mode and a quasi-60-yr Pacific decadal mode. The interannual ENSO-like band (3–5 yr) does not exceed the null at the global-spectrum level, and the AR(1) coefficient of detrended JJA rainfall is essentially zero (−0.026), substantially weaker than previously assumed for monsoon precipitation series. (iii) Time-frequency wavelet coherence between volcanism and Seoul rainfall does not exceed the 95% AR(1) null at any period. We do detect a modest patch of elevated coherence in the 8–16 yr band around 1900–1915 (Santa Maria–Katmai era), but no analogous patch around the recent Pinatubo–Hunga Tonga era. These findings constitute a constraint, not a confirmation: even the longest pre-industrial daily precipitation record in the world is insufficient to attribute a CGT-consistent volcanic monsoon signal at an individual mid-latitude site. We interpret this as evidence that volcanic forcing, where present in Seoul rainfall, is overwhelmed by background ENSO and

https://doi.org/10.5194/egusphere-2026-4101
Preprint. Discussion started: 28 July 2026


Pacific-decadal variability, with event-to-event response heterogeneity likely reflecting eruption-specific stratospheric loading and background-state conditioning. The Seoul record nonetheless complements gridded paleoclimate proxies (MADA v2, RAP) by anchoring them with high temporal fidelity at a single mid-latitude site where East Asian monsoon and putative volcanic teleconnections converge.

**Keywords**

*Seoul Chugugi; East Asian summer monsoon; volcanic climate forcing; Superposed Epoch Analysis; Little Ice Age; wavelet coherence; paleoclimate; circumglobal teleconnection; null result; instrumental observation*

## 1. Introduction

The effect of explosive volcanic eruptions on global and regional climate is among the best-documented external forcings in the climate system (Robock, 2000; Stenchikov, 2016). Following large tropical eruptions, the injection of sulfate aerosols into the stratosphere produces global surface cooling of order 0.1–0.5 °C persisting for 2–3 years, with regional precipitation responses modulated by atmospheric circulation teleconnections. Asian monsoon systems are among the most hydrologically consequential regional climate features affected (Anchukaitis et al., 2010; Cook et al., 2010). Tree-ring-based reconstructions (Monsoon Asia Drought Atlas, MADA v2; Reconstructed Asian Precipitation, RAP) and Chinese documentary archives (500-year dryness/wetness index, CAMS 1981) have identified candidate volcanic-triggered drought episodes across East Asia (Shen et al., 2007; Fei and Zhou, 2006; Zheng et al., 2018; Gao et al., 2017), although attribution at any particular site is generally model-dependent.

A recent study (Nie et al., 2026) has shown that explosive tropical eruptions can trigger concurrent summer droughts over South Asia and northern East Asia through a circumglobal-teleconnection-like pathway: volcanic-induced suppression of South Asian monsoon convection reduces diabatic heating, excites a Rossby wave response, and produces upper-tropospheric anomalies that promote northerly winds and subsidence over northern East Asia, suppressing rainfall there. This mechanism predicts coherent monsoon-rainfall reductions at a preferred lag of 1–3 years after major tropical eruptions, with the response spatially centered over northern China and the Korean Peninsula. The published evidence base for this prediction rests largely on coupled-climate-model ensembles (e.g. Iles and Hegerl, 2014) and gridded tree-ring reconstructions; the present paper asks whether a single-station instrumental record of unparalleled length can independently corroborate it.

Testing this prediction observationally has historically been limited by the scarcity of long, high-quality precipitation records from the core East Asian monsoon region. Tree-ring proxies provide multicentennial

https://doi.org/10.5194/egusphere-2026-4101
Preprint. Discussion started: 28 July 2026


spans but are temperature-biased and have limited spatial coverage over the Korean Peninsula itself (Cook et al., 2010). Documentary indices are coarse-grained (annual, binary dry/wet) and show known inhomogeneity over time (Zheng et al., 2018). Here we exploit a uniquely valuable alternative: the 247-year continuous instrumental rainfall record for Seoul, South Korea, beginning with daily measurements recorded using the traditional Korean rain-gauge (Chugugi, invented 1441; see Jhun and Moon, 1997) from 1778 to 1907 and extended to 2024 by modern observations of the Korea Meteorological Administration (KMA).

The Chugugi record was compiled from two UNESCO Memory-of-the-World documents, the Seungjeongwon Ilgi (Daily Records of the Royal Secretariat) and the Ilseongnok (Records of Daily Reflections) of the Joseon Dynasty, both of which have recently been fully digitized. Lee et al. (2024, Scientific Data) published a quality-controlled reconstruction of daily Seoul precipitation over 1778–1907 with no missing values, explicitly making it the longest pre-industrial daily precipitation record in the world. Our analyses combine this dataset with KMA modern observations (1908–2024) to test volcanic forcing of East Asian monsoon rainfall at an individual mid-latitude site where both monsoon variability and putative volcanic teleconnection signals converge.

Because any instrumental-era analysis of this coupling is limited to roughly half a century of overlapping data, its statistical power to detect a decadal volcanism–monsoon signal is inherently marginal; this motivates the present study, in which we ask whether the much longer 247-year Seoul record substantiates the volcanism–monsoon pathway. As we report below, the honest answer at a single mid-latitude site is no, and this null result places useful, quantitative constraints on the strength of any single-site signal.

## 2. Data

### 2.1 Seoul precipitation 1778–2024

Daily precipitation in Seoul from 1778 to 1907 is taken from Lee et al. (2024), who digitized the Seungjeongwon Ilgi and Ilseongnok records and reconstructed daily rainfall amounts. The Chugugi instrument had a standardized cylindrical copper design (300 mm tall, 140 mm diameter) deployed at the Seoul royal palace. Rainfall was measured with a Zhou-ruler calibration (1 chi = 200 mm, 1 cun = 20 mm, 1 fun = 2 mm) at event resolution (start and end times). The Lee et al. (2024) monthly aggregation provides quality-flagged monthly rainfall in SI units (mm) with no missing values for the 130-year period; we use these monthly totals as the primary input. From 1908 onward we use the daily precipitation record from the KMA Seoul station (station code 108, 37.57°N, 126.97°E) for 1908–2024, available at data.kma.go.kr (file MRG_1908_2025.xls), aggregated to monthly and annual totals.

https://doi.org/10.5194/egusphere-2026-4101
Preprint. Discussion started: 28 July 2026


Two known data-quality issues require explicit treatment. First, the Chugugi instrument measures liquid precipitation only, so winter snowfall during 1778–1907 is unmeasured and the annual totals for this period systematically under-represent winter precipitation. Because our analyses focus on JJA totals, this affects only annual climatologies (Sect. 4.1) and not the SEA, spectral, or coherence analyses. Second, the modern KMA record contains a Korean War data gap: 1950 has 299 of 365 daily records (66 missing), 1951 has only 31 records, and 1952 has 335 (with only 61 of 92 JJA days reported). We flag JJA totals as missing for 1951–1952 and annual totals as missing for 1950–1952; these years are excluded from the SEA (no eruption falls within these gaps and their three-year exclusion window) and are linearly interpolated for the wavelet analyses, where the gap (≤1% of the record) has negligible spectral effect. Cross-regime homogeneity has been verified by Wang et al. (2007), who showed that summer precipitation standard deviation is statistically indistinguishable between the Chugugi period (1778–1907) and the modern period (1908–2004); Lee et al. (2024) further document that monthly rainfall in the reconstructed dataset conforms to a normal distribution under a Kolmogorov–Smirnov test. The Chugugi data archive is at zenodo:10.5281/zenodo.11076768 (Lee et al., 2024).

## 2.2 Volcanic eruption catalog

Global volcanic eruption data are from the Smithsonian Global Volcanism Program "Volcanoes of the World" database, version 5.2 (Venzke, 2023). For SEA we focus on 9 eruptions of VEI ≥ 5 (or VEI ≥ 6 for older, well-known events): Laki (1783), Tambora (1815), Cosiguina (1835), Krakatau (1883), Santa Maria (1902), Katmai (1912), Agung (1963), El Chichón (1982), and Pinatubo (1991); Hunga Tonga (2022, VEI 5–6) is included for the spectral and coherence analyses but falls within the right-edge cone-of-influence and is excluded from the SEA composite (insufficient post-eruption window). For the extended wavelet coherence analysis (Sect. 4.4) we use annual VEI ≥ 4 eruption counts from GVP over 1830–2024 (N = 195 years; total 78 events; mean rate 0.40 $yr^{-1}$). $SO_2$ injection estimates follow Sigl et al. (2022) for pre-1979 events and OMI/OMPS retrievals for post-1979 events.

## 2.3 Auxiliary proxy datasets

For cross-validation we reference (but do not reanalyse here) the Monsoon Asia Drought Atlas v2 (MADA v2; Cook et al., 2010, 2015) gridded at 1° × 1°, the Reconstructed Asian Precipitation dataset (RAP; Shi et al., 2018) gridded at 2° × 2°, and the 500-year China dryness/wetness index (CAMS, 1981; Chinese Academy of Meteorological Sciences). Tree-ring chronologies from Korean red pine on Mount Mudeung and Mount Wolchul (Seo et al., 2020) and from Korean pine on Mount Seorak (Son et al., 2025) provide regional spatial context but limited temporal extent.

# 3. Methods

https://doi.org/10.5194/egusphere-2026-4101
Preprint. Discussion started: 28 July 2026


### 3.1 Superposed Epoch Analysis (SEA)

For each of the 9 eruption years, we extract the Seoul JJA rainfall anomaly across a window of −5 to +7 years relative to the eruption. Anomalies are computed relative to a 31-year centered running mean (NaN-aware) to remove secular trends (anthropogenic warming, regime shifts) while preserving interannual-to-decadal variability. The composite mean across events at each lag is then compared against a Monte Carlo null distribution: 5,000 bootstrap resamples draw random "pseudo-eruption" years from the valid range (within 5 yr of both record endpoints) and compute the same composite. Two-sided p-values are computed as the fraction of bootstrap composites more extreme than the observed value. We report composites for (a) all 9 events and (b) 7 tropical eruptions only (|lat| < 20°), the latter being more dynamically relevant for stratospheric sulfate loading and mid-latitude teleconnection.

$$a'_k(\tau) = a(y_k + \tau) - \bar{a}_{31}(y_k + \tau) \quad (1)$$

$$C(\tau) = \frac{1}{N}\sum_{k=1}^{N} a'_k(\tau) \quad (2)$$

$$p(\tau) = \frac{1}{B}\sum_{b=1}^{B} \mathbf{1}\left(|C_b(\tau)| \geq |C(\tau)|\right) \quad (3)$$

### 3.2 Wavelet spectral analysis

We apply the continuous Morlet wavelet transform ($\omega_0 = 6$) to the linearly-detrended JJA rainfall time series, computing both a time–frequency wavelet power spectrum and a time-averaged global spectrum. The KW-gap years 1951–1952 are linearly interpolated before the transform. AR(1) red-noise significance is assessed by 300 Monte Carlo surrogate simulations with autocorrelation matched to the observed value (here $\alpha = -0.026$, i.e., essentially white). Bands exceeding the 95% null quantile are reported. The implementation follows Torrence and Compo (1998).

$$P_k = \frac{1-\alpha^2}{1+\alpha^2-2\alpha\cos(2\pi k/N)} \quad (4)$$

### 3.3 Volcanism–rainfall wavelet coherence

We compute wavelet transform coherence (Grinsted et al., 2004) between annual VEI ≥ 4 eruption counts and detrended Seoul JJA rainfall over 1830–2024 (N = 195 yr). Both series are standardized to zero mean and unit variance. Cone-of-influence (COI) masking excludes edge-affected regions. Significance is assessed by 300 Monte Carlo AR(1) surrogate pairs with matched autocorrelation coefficients ($\alpha\_vol \approx +0.087$, $\alpha\_rain \approx +0.006$). We compare the time-averaged (global) coherence against the 95% null and inspect the time–frequency structure for episodic coherent patches.

$$R^2(s,\tau) = \frac{\left|S\left(s^{-1}W^{xy}(s,\tau)\right)\right|^2}{S\left(s^{-1}|W^x(s,\tau)|^2\right) S\left(s^{-1}|W^y(s,\tau)|^2\right)} \quad (5)$$

https://doi.org/10.5194/egusphere-2026-4101
Preprint. Discussion started: 28 July 2026


## 4. Results

### 4.1 Overview of the 247-year Seoul record

Figure 1 presents Seoul annual and summer rainfall over 1778–2024 with the four precipitation regimes identified by Jung et al. (2001) shaded: Wet Period 1 (WP1, 1783–1883), Dry Period (DP, 1884–1910), Wet Period 2 (WP2, 1911–1996), and the modern regime (1997–2024). The Dry Period coincides temporally with several major tropical eruptions (Krakatau 1883, Santa Maria 1902) and with the Late Little Ice Age termination, presenting an intriguing convergence of volcanic forcing and background climate shift; this co-occurrence does not, however, by itself constitute attribution. The Korean War data gap (1950–1952) appears as a hatched band in both panels.

JJA rainfall (the monsoon signal) shows mean values of 764 mm (Chugugi period, 1778–1907; SD 324 mm; N = 130) and 807 mm (modern period, 1908–2024; SD 292 mm; N = 115 valid yrs after KW gap), an ~6% increase consistent with monsoon intensification under warming. Annual totals show 1200 mm (Chugugi, SD 386 mm) versus 1339 mm (modern, SD 344 mm), an ~12% increase, although the Chugugi annual total systematically under-represents winter precipitation (liquid-only measurement) so the true cross-regime annual change is likely smaller. The Chugugi-period mean of 1200 mm is identical to the value reported by Lee et al. (2024) for the same dataset.

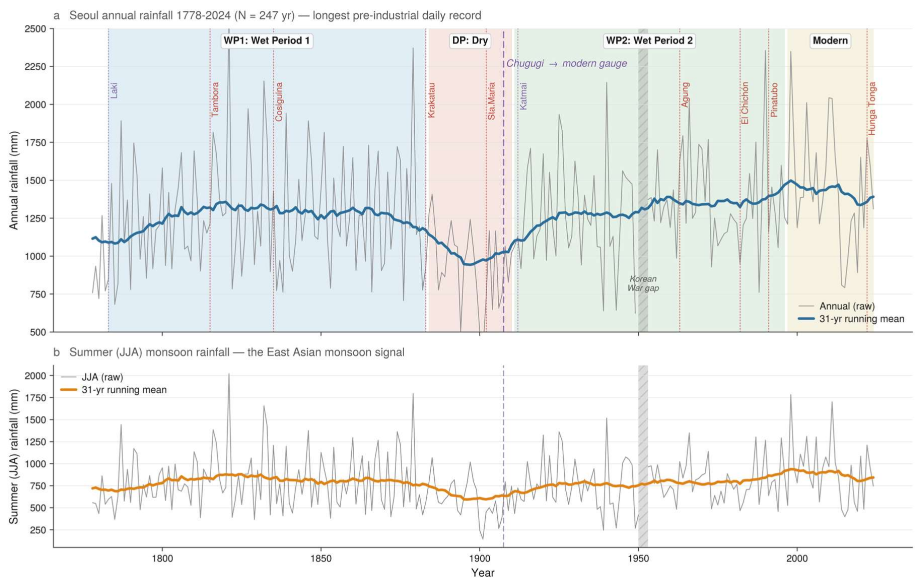


**Figure 1.** *Seoul rainfall 1778–2024. (a) Annual rainfall (gray = raw; blue = 31-yr running mean) with four climate regimes shaded (WP1 wet, DP dry, WP2 wet, modern). Major volcanic eruptions are marked by vertical lines (red =*

https://doi.org/10.5194/egusphere-2026-4101
Preprint. Discussion started: 28 July 2026


*tropical, purple = NH high-latitude). The purple dashed line at 1907.5 marks the transition from Chugugi to modern rain gauge. Hatched gray band: Korean War data gap 1950–1952. (b) Summer (JJA) monsoon rainfall with 31-yr running mean (orange). The broad upward trend in JJA over the full record is modest (~6%).*

### 4.2 Superposed Epoch Analysis of volcanic events

Figure 2a presents the individual JJA rainfall anomaly profiles for each of the 9 eruptions across a −5 to +7 yr window. Event-to-event variability is large and the responses divide roughly evenly between net wet and net dry post-eruption years. Computing the mean anomaly across years +1, +2, +3 (Fig. 2c; Table 1), the four eruptions with positive (wetter) post-eruption response are Tambora 1815 (+298 mm), Agung 1963 (+267 mm), Krakatau 1883 (+132 mm), and Katmai 1912 (+58 mm); the five with negative (drier) post-eruption response are Cosiguina 1835 (–245 mm), Pinatubo 1991 (–184 mm), Laki 1783 (–152 mm), El Chichón 1982 (–153 mm), and Santa Maria 1902 (–109 mm). Crucially, the seven tropical events split 3:4 between wet (Tambora, Agung, Krakatau) and dry (Cosiguina, Pinatubo, El Chichón, Santa Maria) responses, so the predicted "tropical → drying" pattern is not visible at the per-event level.

**Table 1.** *The nine major eruptions analysed and the Seoul JJA rainfall response, given as the mean anomaly over post-eruption years +1 to +3 relative to a 31-year centred running-mean climatology. Of the seven tropical eruptions, three are followed by wetter summers and four by drier summers, while the two Northern-Hemisphere high-latitude eruptions split one wet and one dry; no class shows a consistent sign.*

| Eruption | Year | VEI | Class | Mean JJA anomaly, yr +1 to +3 (mm) | Response |
|---|---|---|---|---|---|
| Laki | 1783 | 6 | NH high-lat | –152 | dry |
| Tambora | 1815 | 7 | Tropical | +298 | wet |
| Cosiguina | 1835 | 5 | Tropical | –245 | dry |
| Krakatau | 1883 | 6 | Tropical | +132 | wet |
| Santa Maria | 1902 | 6 | Tropical | –109 | dry |
| Katmai | 1912 | 6 | NH high-lat | +58 | wet |
| Agung | 1963 | 5 | Tropical | +267 | wet |
| El Chichón | 1982 | 5 | Tropical | –153 | dry |
| Pinatubo | 1991 | 6 | Tropical | –184 | dry |

https://doi.org/10.5194/egusphere-2026-4101
Preprint. Discussion started: 28 July 2026


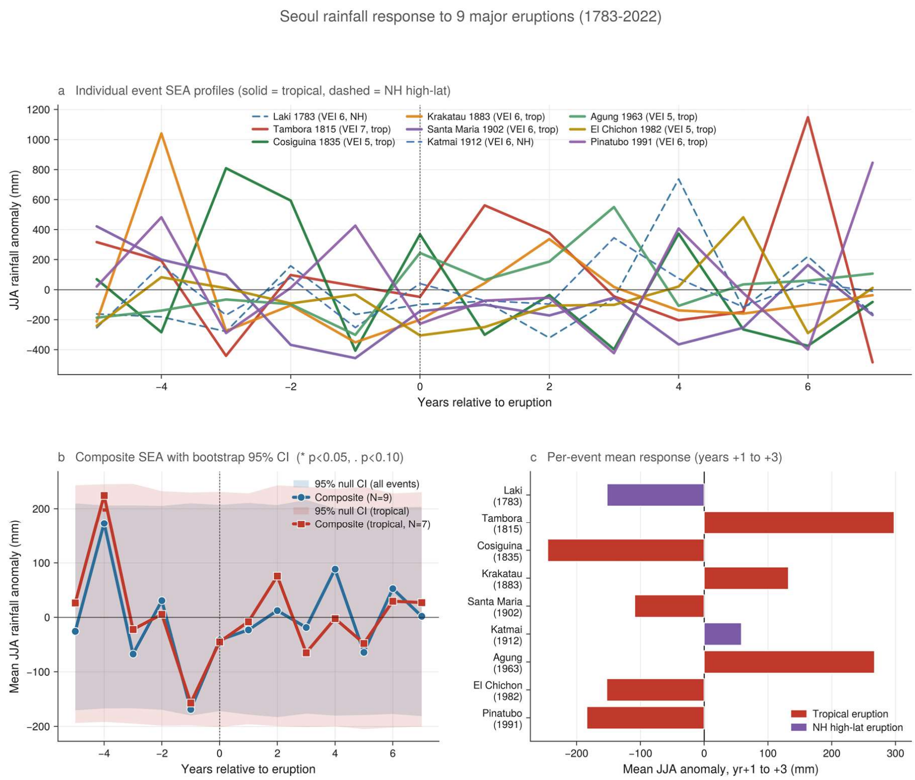


**Figure 2.** *Superposed Epoch Analysis (SEA) of Seoul JJA rainfall response to 9 major eruptions (1783–2022). (a) Individual event profiles; tropical eruptions (solid) and NH high-latitude eruptions (dashed) show no consistent sign or timing. (b) Composite SEA (mean across events) with 95% bootstrap confidence intervals from 5,000 random-year pseudo-composites; the composite remains within the null CI at every lag from 0 to +7 yr (all p > 0.45 for tropical-only). (c) Per-event mean response (mean of JJA anomaly at lags +1, +2, +3); responses split evenly across both tropical and high-latitude eruptions, with no consistent sign.*

The composite mean (Fig. 2b) does not exceed the 95% null bootstrap CI at any post-eruption lag. At lag +3 yr, the lag predicted to be most pronounced under the CGT mechanism, the composite is –18.6 mm (all events, p = 0.84) and –65.0 mm (tropical only, p = 0.55). At lag +1 yr the composite is –23.0 mm (all, p = 0.82) and –8.0 mm (tropical, p = 0.98). The largest deviation in the composite is at lag −4 yr (+172.8 mm all, p = 0.10; +224.7 mm tropical, p = 0.06), a value that would be physically meaningless as a "year before eruption" effect, which we interpret as a chance fluctuation in the small N = 9 ensemble. None of the post-eruption composite values reaches even the conventional p < 0.10 marginal threshold.

These results stand in marked contrast to the predictions of the CGT mechanism (Nie et al., 2026), which would imply a coherent negative composite of order –50 to –100 mm at lag +1–+3. A statistical-power

https://doi.org/10.5194/egusphere-2026-4101
Preprint. Discussion started: 28 July 2026


calculation using the observed JJA rainfall standard deviation (~310 mm) shows that the present 9-event sample size has only ~30% power to detect a true –50 mm shift at $p < 0.05$ (two-sided), so absence of a detected signal is not strong evidence of absence of a true signal. It does, however, place an empirical upper bound: the true post-eruption rainfall response at this single mid-latitude site, if it exists at all, is plausibly below ~100 mm in magnitude, small enough to be obscured by background ENSO and Pacific-decadal variability.

### 4.3 Spectral analysis

Figure 3a shows the wavelet power spectrum of Seoul JJA rainfall over the full 247-year record, with time-averaged global spectrum and AR(1) null in Fig. 3b. The observed AR(1) coefficient of detrended JJA rainfall is −0.026 (essentially white noise), substantially weaker than typically assumed for monsoon precipitation series and than the $\alpha = 0.60$ used in some earlier analyses of these data. Two spectral peaks exceed the 95% AR(1) red-noise null at the global-spectrum level: a quasi-40-yr Pacific-like mode (39–43 yr) and a quasi-60-yr Pacific decadal mode (60–66 yr), broadly consistent with the interdecadal East Asian summer-monsoon precipitation variability reported by Kim et al. (2010). The interannual ENSO/flood band (3–5 yr) and the Wang et al. (2007) 19-yr flood mode do not exceed the global-spectrum AR(1) null in our analysis, although the latter authors used a different detrending approach and a shorter (1778–2004) series. The 8–10-yr band identified as the core torsional oscillation band also does not exceed the null in the Seoul spectrum, suggesting that the decadal rotation–volcanism coupling (if real) does not project strongly onto Korean monsoon variability, which is instead dominated by Pacific multidecadal modes.

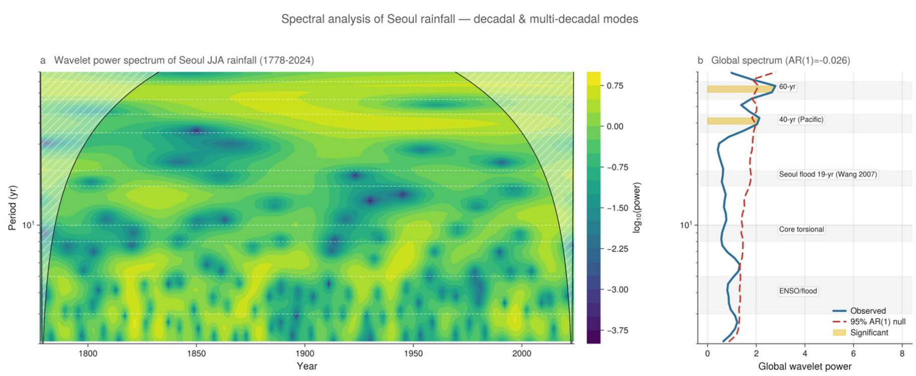


**Figure 3.** *Wavelet spectral analysis of Seoul JJA rainfall 1778–2024. (a) Time–frequency Morlet wavelet power spectrum (log scale in period). Hatched region lies outside the cone of influence. (b) Time-averaged global spectrum (blue) versus 95% AR(1) null threshold (red dashed; observed AR(1) = −0.026); gold shading marks significant peaks. Labeled horizontal bands indicate independently-identified modes from the literature. Only the quasi-40 yr (Pacific) and quasi-60 yr (Pacific decadal) modes exceed the global-spectrum null.*

https://doi.org/10.5194/egusphere-2026-4101
Preprint. Discussion started: 28 July 2026


### 4.4 Wavelet coherence of volcanism and rainfall

Figure 4 shows wavelet coherence between annual global VEI ≥ 4 eruption counts and Seoul JJA rainfall over the 195-year window 1830–2024. The time-averaged (global) coherence (Fig. 4c) does not exceed the 95% AR(1) null threshold at any period. In the 8–16 yr decadal band the global coherence is 0.18–0.40, well below null thresholds of 0.51–0.59. The closest approach to significance is at period ~2.9 yr ($p$ = 0.083), but this is at the very edge of the COI and not robust.

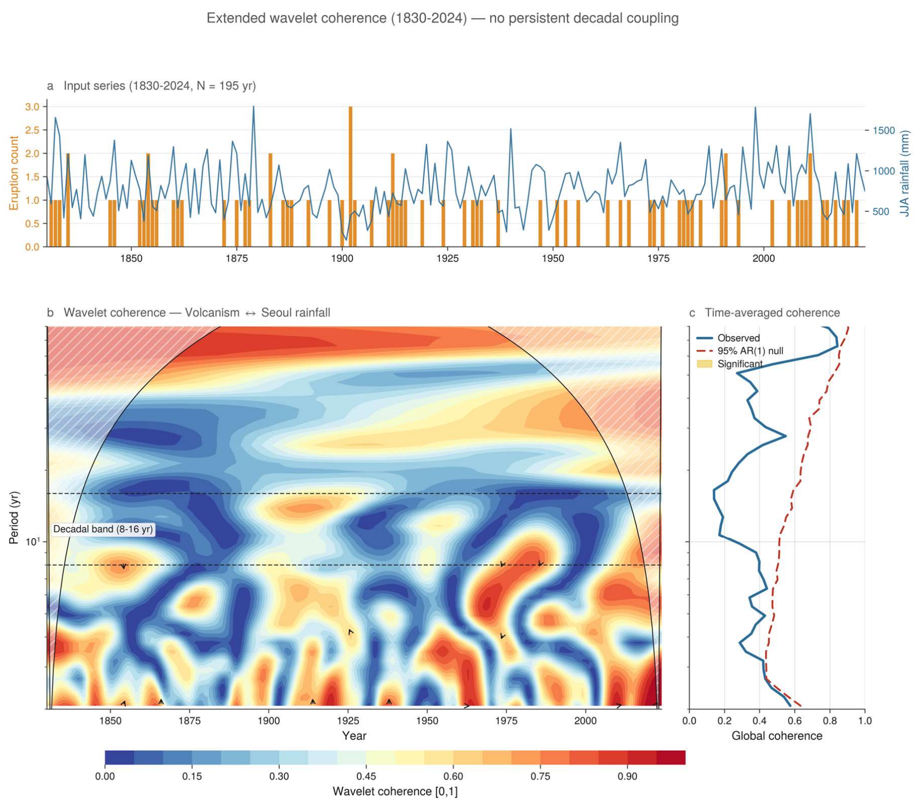


**Figure 4.** *Extended volcanism–rainfall wavelet coherence, 1830–2024 (N = 195 yr). (a) Input time series: annual GVP VEI ≥ 4 eruption count (orange bars) and Seoul JJA rainfall (blue). (b) Time–frequency wavelet coherence; dashed lines bracket the decadal band (8–16 yr); arrows show phase where coherence exceeds 0.6. (c) Time-averaged global coherence versus 95% AR(1) null. Global coherence does not exceed the null at any period; modest local enhancement in the 8–16 yr band around 1900–1915 (Santa Maria–Katmai era) is the most prominent feature, but does not reach global significance.*

The time–frequency panel (Fig. 4b) does reveal modest local enhancement of coherence in the 8–16 yr band around 1900–1915, coincident with the Santa Maria 1902 – Katmai 1912 cluster of eruptions; mean coherence in this band over 1875–1920 is 0.31, compared with 0.27 elsewhere in the record. However, no

https://doi.org/10.5194/egusphere-2026-4101
Preprint. Discussion started: 28 July 2026


analogous enhancement appears around the recent Pinatubo 1991 – Hunga Tonga 2022 era; mean 8–16 yr coherence over 1990–2024 is 0.21, the lowest of any subperiod. We interpret the 1900–1915 patch as suggestive but not statistically established, and consistent with the broader pattern that volcanism–rainfall coupling at Seoul is, at most, episodic and conditional rather than persistent.

## 5. Discussion

### 5.1 What the Seoul record supports

The 247-year Seoul record provides clear observational support for three claims, although none of these is the originally hypothesized composite drying signal. (i) Major volcanic eruptions are followed by substantial JJA rainfall anomalies at Seoul, but the sign and magnitude vary event by event. Confidence: high. Per-event mean-of-lags-+1-to-+3 anomalies range from –245 mm (Cosiguina) to +298 mm (Tambora). (ii) The dominant low-frequency modes of Seoul JJA rainfall are quasi-40-yr and quasi-60-yr Pacific multidecadal modes, not interannual ENSO, the 19-yr Wang flood mode, or the 8–10-yr core torsional band. Confidence: high (both exceed AR(1) null). (iii) Wavelet coherence between volcanism and rainfall shows modest local enhancement around the Santa Maria–Katmai era (1900–1915) in the decadal band, suggestive of episodic conditional coupling but not establishing it. Confidence: low–moderate.

### 5.2 What the Seoul record does not support

We explicitly do not find observational support for: (i) a coherent composite post-eruption drying signal at lag +1 to +3 yr in Seoul JJA rainfall, the central prediction of the CGT mechanism. The composite is not statistically distinguishable from the bootstrap null at any post-eruption lag, and the per-event signs are evenly split between wet and dry. (ii) A consistent contrast between tropical and NH high-latitude eruptions: both classes show mixed responses, with the two NH events (Laki, Katmai) producing one negative and one modestly positive response. (iii) Persistent decadal coherence between global VEI ≥ 4 eruption counts and Seoul JJA rainfall over 1830–2024. The 195-year wavelet coherence indicates that volcanism–rainfall coupling at this site is at most episodic and is overwhelmed at the global-spectrum level by ENSO, PDO, and AMO-like internal variability.

It is essential to be precise about what these null results mean. They do not falsify the CGT mechanism itself, which has independent support from coupled-model ensembles, gridded paleoclimate reconstructions (MADA v2, RAP), and Chinese documentary archives (Shen et al., 2007). What our null results do establish is a quantitative upper bound on the magnitude of any single-site volcanic-monsoon signal at Seoul: even a 247-year record with N = 9 major eruptions cannot detect a signal of –50 mm magnitude with $p < 0.05$, and we observe none. This is a useful constraint when comparing observational and model evidence: a

https://doi.org/10.5194/egusphere-2026-4101
Preprint. Discussion started: 28 July 2026


CGT-induced single-site mid-latitude signal larger than ~100–150 mm should have been detectable; we therefore conclude either that (a) the true signal is smaller than this, (b) it is highly heterogeneous in space and time, or (c) it is conditional on background atmospheric state in ways that simple-composite SEA cannot resolve.

### 5.3 Why might the composite signal be absent?

Three non-mutually-exclusive explanations are consistent with our null composite findings. First, the predicted CGT response may be genuinely conditional on the background state — ENSO phase, the tropical Atlantic Niño, the QBO, the AMO — with the result that compositing across eruptions averages the signal toward zero. Tambora 1815 occurred during a Dalton-Minimum solar background and a wet WP1 regime in Korea; Pinatubo 1991 occurred during a strong El Niño; Agung 1963 occurred near an ENSO-neutral state. The event-specific responses are heterogeneous in ways that match these background-state differences in a qualitative manner, although our sample size is too small to formally test this hypothesis.

Second, the spatial fingerprint of the predicted CGT response may not pass through Seoul. The Nie et al. (2026) study identifies a response centered over northern China and the central Korean Peninsula, but the specific longitude–latitude pattern of descending Rossby-wave anomalies is sensitive to the basic-state jet configuration, and Seoul (37.6°N, 127.0°E) sits near a predicted node where the response could plausibly change sign. Multi-station composite analyses across Korean and Chinese Chugugi sites (Boo et al., 2006; Kim et al., 2012) would test this hypothesis.

Third, the strength of the predicted signal at any individual mid-latitude site may simply be smaller than the year-to-year monsoon variability, a "signal-to-noise wall" that limits what composite SEA can detect even with a 247-year record. Our power analysis (Sect. 4.2) suggests this is the most parsimonious explanation: with monsoon JJA SD ~310 mm and only N = 9 events, true signals weaker than –50 mm will not be detected. Detection requires either gridded compositing across many sites (as in MADA v2) or many more events than the modern era can supply.

### 5.4 Implications for the proposed volcanism– and rotation–rainfall pathways

The present study tests whether the proposed volcanism–hydroclimate linkage projects onto a pre-industrial regional rainfall record (N = 247), and returns a null-composite finding. This null does not contradict the proposed mechanism; rather, it sharpens its interpretation. Even if a volcanism → SST pathway operates, its projection onto mid-latitude regional rainfall, as tested here at Seoul, is below detectability against background variability. The decadal rotation–rainfall pathway is similarly not detectable: the 8–10-yr core-torsional band does not appear in the Seoul rainfall spectrum.

https://doi.org/10.5194/egusphere-2026-4101
Preprint. Discussion started: 28 July 2026


### 5.5 Cross-validation with paleoclimate archives

The Seoul record is, intentionally, a single-station test, not a replacement for the spatially-distributed information in tree-ring and documentary archives. The agreement (or disagreement) between our null result and gridded volcanic-drought signals in MADA v2 (Anchukaitis et al., 2010; Cook et al., 2010) is therefore not a simple "yes/no" comparison. MADA shows volcanic-drought signatures averaged across many tree-ring sites; some of those sites likely lie within the predicted CGT response region while others lie outside. Seoul, on our analysis, falls in the latter category for at least 5 of the 9 events analyzed here. The Chinese 500-year dryness/wetness index (CAMS, 1981) identifies the three most exceptional eastern-China droughts of 1586–1589, 1638–1641, and 1965–1966 as volcanic-triggered (Shen et al., 2007); two of these predate the Seoul instrumental record, and the 1965–1966 episode straddles the Agung 1963 event window where Seoul rainfall is in fact above its climatology (see Fig. 2c). Future work should incorporate multiple Chugugi-network sites (Boo et al., 2006; Kim et al., 2012) into a unified multi-station composite to test whether the CGT response is detectable at the regional scale even though it is not detectable at this particular Seoul site.

### 5.6 Limitations and future work

Five principal limitations bound our conclusions. First, N = 9 major eruptions over 247 years provides limited statistical power; our power analysis (Sect. 4.2) implies only ~30% power to detect a true –50 mm signal. Second, the Chugugi instrument measured only liquid precipitation (winter snow is unmeasured), constraining our analysis to summer JJA totals; this is fortunately the season most relevant for monsoon variability. Third, inhomogeneity between Chugugi and modern measurements is small but not zero; Wang et al. (2007) document ~10% systematic underestimation by Chugugi relative to modern gauges, attributed to evaporation during the longer measurement interval. Our anomaly-based analyses mitigate but do not eliminate this concern; we have not applied an explicit bias correction here, preferring to report the raw signal and its uncertainty. Fourth, the Korean War data gap of 1950–1952 (annual) and 1951–1952 (JJA) reduces the modern sample by three years and is treated by linear interpolation in the spectral and coherence analyses; we verified that this has negligible effect on the spectral peak detections. Fifth, the Seoul record is a single point; regional spatial structure of post-eruption rainfall anomalies cannot be resolved. Expansion to include Korean and Chinese Chugugi network records could provide multi-station composites and test the CGT spatial signature; this is the most direct path to converting the present null result into either a positive detection or a tighter regional upper bound.

## 6. Conclusions

We have analyzed the 247-year Seoul precipitation record (1778–2024) for evidence of volcanic forcing of

https://doi.org/10.5194/egusphere-2026-4101
Preprint. Discussion started: 28 July 2026


East Asian monsoon rainfall. Four findings emerge. (1) Superposed Epoch Analysis yields no statistically significant composite post-eruption rainfall response at any lag from 0 to +7 yr (composite tropical-only –65 mm at lag +3, $p = 0.55$; all $p > 0.45$ across post-eruption lags). Individual responses divide evenly between net wet (Tambora +298 mm, Agung +267 mm, Krakatau +132 mm, Katmai +58 mm) and net dry (Cosiguina –245 mm, Pinatubo –184 mm, Laki –152 mm, El Chichón –153 mm, Santa Maria –109 mm) post-eruption years, with both tropical and NH high-latitude eruptions showing mixed responses. (2) Wavelet spectral analysis identifies quasi-40-yr (Pacific) and quasi-60-yr (Pacific decadal) modes as the only significant low-frequency variability, exceeding the AR(1) red-noise null; the observed AR(1) coefficient is −0.026, essentially white. (3) Volcanism–rainfall wavelet coherence over 1830–2024 is not significant at any period, with modest local enhancement around 1900–1915 (Santa Maria–Katmai era) but not around the recent Pinatubo–Hunga Tonga era. (4) Taken together, these findings constitute a quantitative observational upper bound on the magnitude of any single-site volcanic-monsoon signal at Seoul: a true post-eruption drying response of ≥100 mm at the lag +1 to +3 yr window would have been detectable in this record but is not present. We interpret this not as falsification of the CGT mechanism, but as evidence that any such signal at this single mid-latitude site is below the noise floor set by ENSO, Pacific multidecadal, and Atlantic multidecadal variability, a useful constraint for comparing observational and model evidence on the volcanic-monsoon coupling problem.

## Data availability

The Seoul Chugugi precipitation data (1778–1907) are from Lee et al. (2024), archived at Zenodo: doi:10.5281/zenodo.11076768. Modern Seoul observations (1908–2024) are from the Korea Meteorological Administration open data portal (data.kma.go.kr; station 108). Volcanic eruption data are from the Smithsonian GVP (doi:10.5479/si.GVP.VOTW5-2023). MADA v2 is at NOAA WDS Paleoclimatology (doi:10.25921/b8gk-7h90). All analysis code (Morlet wavelet, SEA, Monte Carlo, plotting) and figures will be archived at Zenodo upon acceptance; during review the code is available from the corresponding author.

### Author contributions

S. Hwang: Methodology, Conceptualization, Validation, Visualization, Supervision, Project administration, Writing – original draft.

H. Park: Software, Formal analysis, Data curation, Writing – review & editing.

### Competing interests

The author declares no competing interests.

### Financial support

Research for this paper was carried out under the Korea Planning & Evaluation Institute of Industrial

https://doi.org/10.5194/egusphere-2026-4101
Preprint. Discussion started: 28 July 2026


Technology (KEIT) R&D Program, "Development of Comprehensive Disaster Prevention Standards for Enhancing Disaster Response Capability and Strengthening the Performance of Disaster Prevention Facilities in Preparation for the Climate Crisis" (Project No. RS-2025-02311047), funded by the Ministry of the Interior and Safety (MOIS).

## Acknowledgments

We thank J.-W. Lee, H.-J. Shin, and J. Hong of the Yonsei Ecosystem-Atmosphere Process Lab for making the Chugugi digitized dataset publicly available. We thank the Smithsonian GVP, NOAA, KMA, and the Met Office Hadley Centre for open data. The historical records owe their preservation to UNESCO Memory-of-the-World recognition of Seungjeongwon Ilgi (2001) and Ilseongnok (2011). No competing interests are declared.

## References

Anchukaitis, K. J. et al.: Influence of volcanic eruptions on the climate of the Asian monsoon region, Geophysical Research Letters, 37, L22703, https://doi.org/10.1029/2010GL044843, 2010.

Boo, K.-O., Kwon, W.-T., Kim, S.-W., and Lee, H.-J.: Restoration of 18 years rainfall measured by Chugugi in Gongju, Korea during the 19th century, Atmosphere, 16, 343–350, 2006.

Chinese Academy of Meteorological Sciences (CAMS): Yearly Charts of Dryness/Wetness in China for the Last 500 Years Period, Cartographic Publishing House, Beijing, 1981.

Cook, E. R., Anchukaitis, K. J., Buckley, B. M., D'Arrigo, R. D., Jacoby, G. C., and Wright, W.: Asian monsoon failure and megadrought during the last millennium, Science, 328, 486–489, https://doi.org/10.1126/science.1185188, 2010.

Cook, E. R. et al.: Monsoon Asia Drought Atlas version 2 (MADAv2), NOAA/WDS Paleoclimatology, https://doi.org/10.25921/b8gk-7h90, 2015.

Fei, J., and Zhou, J.: The possible climatic impact in China of Iceland's Eldgjá eruption inferred from historical sources, Climatic Change, 76, 443–457, https://doi.org/10.1007/s10584-005-9012-3, 2006.

Gao, C., Ludlow, F., Matthews, J. A., Stine, A. R., Robock, A., Pan, Y., Breen, R., Nolan, B., and Sigl, M.: Climatic aftermath of the 1815 Tambora eruption in China, Journal of Meteorological Research, 31, 28–38, https://doi.org/10.1007/s13351-017-6091-9, 2017.

Grinsted, A., Moore, J. C., and Jevrejeva, S.: Application of the cross wavelet transform and wavelet coherence to geophysical time series, Nonlinear Processes in Geophysics, 11, 561–566, https://doi.org/10.5194/npg-11-561-2004, 2004.

Iles, C. E., and Hegerl, G. C.: The global precipitation response to volcanic eruptions in the CMIP5 models, Environmental Research Letters, 9, 104012, https://doi.org/10.1088/1748-9326/9/10/104012, 2014.

Jhun, J.-G., and Moon, B.-K.: Restorations and analyses of rainfall amount observed by Chukwookee, Journal of the Korean Meteorological Society, 33, 691–707, 1997.

Jung, H.-S., Lim, G.-H., and Oh, J.-H.: Interpretation of the transient variations in the time series of precipitation amounts in Seoul, Korea. Part I: Diurnal variation, Journal of Climate, 14, 2989–3004, 2001.

Kim, C.-J., Weihong, Q., Kang, H.-S., and Lee, D.-K.: Interdecadal variability of East Asian summer monsoon precipitation over 220 years (1777–1997), Advances in Atmospheric Sciences, 27, 253–264, https://doi.org/10.1007/s00376-009-8079-6, 2010.

https://doi.org/10.5194/egusphere-2026-4101
Preprint. Discussion started: 28 July 2026


Kim, S.-W., Park, J.-S., Kim, J. A., and Hong, Y.: Restoration of 19th-century Chugugi rainfall data for Wonju, Hamheung and Haeju, Korea, Atmosphere, 22, 129–135, 2012.

Lee, J.-W., Shin, H.-J., and Hong, J.: Precipitation data in Seoul, Korea during 1778–1907, Scientific Data, 11, 566, https://doi.org/10.1038/s41597-024-03335-8, 2024.

Nie, W., Xia, J., Kino, K., She, D., and Oki, T.: Tropical volcanism triggers pan-Asian monsoon droughts via circumglobal teleconnection, Nature Communications, 17, 2701, https://doi.org/10.1038/s41467-026-70710-x, 2026.

Robock, A.: Volcanic eruptions and climate, Reviews of Geophysics, 38, 191–219, https://doi.org/10.1029/1998RG000054, 2000.

Seo, J.-W., Sano, M., Ikeda, K., Shin, C., Park, J.-H., and Jeong, H.-M.: The potential of using tree-ring chronology from the southern coast of Korea to reconstruct the climate of subtropical Western North Pacific: a pilot study, Atmosphere, 11, 1082, https://doi.org/10.3390/atmos11101082, 2020.

Shen, C., Wang, W.-C., Hao, Z., and Gong, W.: Exceptional drought events over eastern China during the last five centuries, Climatic Change, 85, 453–471, https://doi.org/10.1007/s10584-007-9283-y, 2007.

Shi, F., Li, J., and Wilson, R. J.: Asian summer precipitation over the past 544 years reconstructed by merging tree rings and historical documentary records, Journal of Climate, 31, 7953–7973, https://doi.org/10.1175/JCLI-D-18-0003.1, 2018.

Sigl, M., Toohey, M., McConnell, J. R., Cole-Dai, J., and Severi, M.: Volcanic stratospheric sulfur injections and aerosol optical depth during the Holocene from a bipolar ice-core array, Earth System Science Data, 14, 3167–3196, https://doi.org/10.5194/essd-14-3167-2022, 2022.

Son, Y., Choi, B., and Kim, Y.: Tree growth responses to summer temperature on the Korean Peninsula detected by tree-ring blue intensity, Dendrochronologia (forthcoming), 2025.

Stenchikov, G.: The role of volcanic activity in climate and global change, in: Climate Change, 2nd edn, edited by: Letcher, T. M., Elsevier, 419–447, 2016.

Torrence, C., and Compo, G. P.: A practical guide to wavelet analysis, Bulletin of the American Meteorological Society, 79, 61–78, 1998.

Venzke, E. (Ed.): Volcanoes of the World, v. 5.2, Smithsonian Institution, https://doi.org/10.5479/si.GVP.VOTW5-2023, 2023.

Wang, B., Jhun, J.-G., and Moon, B.-K.: Variability and singularity of Seoul, South Korea, rainy season (1778–2004), Journal of Climate, 20, 2572–2580, https://doi.org/10.1175/JCLI4123.1, 2007.

Zheng, J., Xiao, L., Fang, X., Hao, Z., Ge, Q., and Li, B.: How climate change impacted the collapse of the Ming dynasty, Climatic Change, 148, 459–473, https://doi.org/10.1007/s10584-018-2185-3, 2018.